Algal Research
January 2023, Volume 69, Pages 102915 (12p.)
https://doi.org/10.1016/j.algal.2022.102915
https://archimer.ifremer.fr/doc/00808/91998/

Light-response in two clonal strains of the haptophyte *Tisochrysis lutea*: Evidence for different photoprotection strategies

Pajot Anne [1, *], Lavaud Johann [2], Carrier Gregory [3], Lacour Thomas [3], Marchal Luc [4], Nicolau Elodie [1]

[1] Ifremer, PHYTOX, GENALG Laboratory, F-44000 Nantes, France
[2] LEMAR, Laboratory of Marine Environmental Sciences, UMR 6539, CNRS/Univ Brest/Ifremer/IRD, Institut Universitaire Européen de la Mer, Technopôle Brest-Iroise, Plouzané, France
[3] Ifremer, PHYTOX, PHYSALG Laboratory, F-44000 Nantes, France
[4] Université de Nantes, GEPEA, F-44000 Saint Nazaire, France

* Corresponding author : Anne Pajot, email address : anne.pajot@gmail.com

Abstract :

To assess the mechanisms of photoprotection in T. lutea, two clonal strains with different basal pigments composition were studied. One synthesized echinenone, while the other did not but showed a high amount of diadinoxanthin and diatoxanthin.

We investigated the photosynthetic response of these two clonal strains in turbidostat, at different growth culture irradiances from 50 to 550 µmol photons m2 s−1. To this end, variable chlorophyll a fluorescence, pigment composition and transcription level of specific genes were monitored. In addition to the genes coding for the Fucoxanthin Chlorophyll a, c binding Protein (FCP), we followed the expression of several putative genes coding for the diadinoxanthin de-epoxidase, the violaxanthin de-epoxidase and the zeaxanthin epoxidase enzymes. It was the first time that these genes were characterized in T. lutea.

Both clonal strains decreased their photosynthetic pigments with increasing irradiance. Nevertheless, the two clonal strains had different photoprotection strategies illustrated with the extent of the dissipation of excess light energy. It was accompanied by the synthesis of photoprotective pigments to different extents: T-5cl6 increased its pool of diadinoxanthin-diatoxanthin with increasing irradiance, while T 4cl3 preferentially synthesized echinenone above a certain level of irradiance. These diverging phenotypes were correlated with variations in the expression of lhcx, lhcr, and of the putative genes of the enzymes involved in the xanthophyll pigment cycles.

Graphical abstract

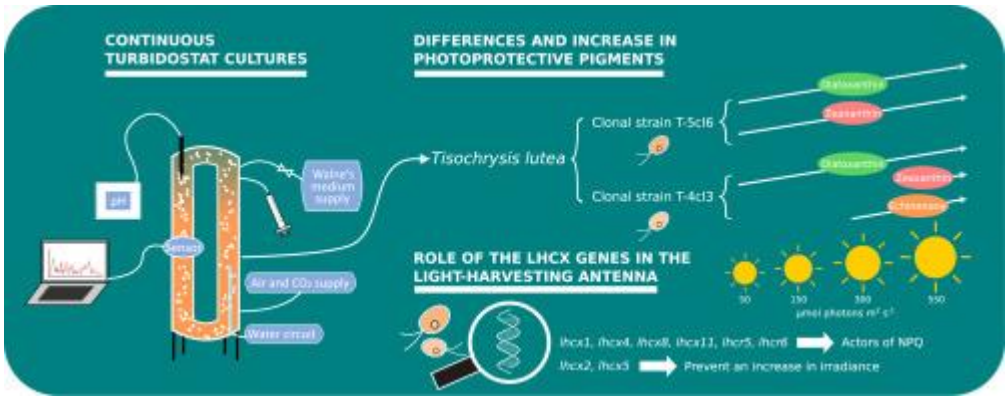

Highlights

► Continuous turbidostat cultures in triplicates were used. ► Two strains of *Tisochrysis lutea* had a different photoprotection strategy. ► Echinenone was remarkably accumulated in one strain under high light. ► Four genes involved in de-epoxidation and epoxidation were annotated. ► *lhcx, lhcr* and *lhcf* participate in the fine photosynthesis/photoprotection balance.

Keywords : Tisochrysis lutea, photoprotection, diatoxanthin, zeaxanthin, echinenone, lhcx

Abbreviations

ROS: reactive oxygen species

LHC: light-harvesting complex

FCP: Fucoxanthin Chlorophyll *a,c* binding Protein

PPF: photosynthetic photon flux, µmol photons m^2 s^{-1}

Ddx: diadinoxanthin

Dtx: diatoxanthin

Vx: violaxanthin

Zx: zeaxanthin

DDE: diadinoxanthin de-epoxidase

VDE: violaxanthin de-epoxidase

ZE: zeaxanthin epoxidase

NPQ: non-photochemical quenching

DES-DD: de-epoxidation state from diadinoxanthin to diatoxanthin

DES-VZ: de-epoxidation state from violaxanthin to zeaxanthin

1. Introduction

Chromista is a well-known clade responsible for 25% of the primary production on Earth [1], composed of brown seaweeds and microalgae, including diatoms and haptophytes. These latter groups are ubiquitous in oceans, and are able to cope with fluctuating light conditions. While performing photosynthesis for their growth, cells have to avoid the photodamages caused by an excess of light energy absorption, generating various reactive oxygen species (ROS) [2,3]. The achievement of an efficient balance between photosynthesis and photoprotection explains part of the worldwide expansion of diatoms and haptophytes [4–6], and they developed several strategies to achieve it. The major player of this very dynamic equilibrium is the light-harvesting antenna, also called the light-harvesting complex (LHC) [7].

The LHC of diatoms and haptophytes, common to all Chromista, is composed of photosynthetic and photoprotective pigments, and of the Fucoxanthin Chlorophyll *a*,*c* binding Protein (FCP) [7]. The FCP is a thylakoid transmembrane protein complex composed of three main protein families. The Lhcf and Lhcr are protein sequences binding mostly photosynthetic pigments such as fucoxanthin (Fx) and chlorophylls (Chl *a* and *c*). The Lhcx bind mostly photoprotective pigments such as diadinoxanthin (Ddx), diatoxanthin (Dtx) [8–10]. It is therefore assumed that Lhcf and Lhcr are related to photosynthesis and Lhcx to photoprotection. However, Lhcf can also bind Ddx, for instance in the diatom *Phaeodactylum tricornutum* [11], highlighting the more complex role of Lhcf within the light-harvesting antenna. Currently in the literature, there is an abundance of studies on the FCP of diatoms [12,13], whereas only a few exist for haptophytes [14,15].

We selected *Tisochrysis lutea* as a representative of haptophyte microalgae, and determined the composition of its FCP in a previous study [15]. 28 Lhcf, 12 Lhcr and 12 Lhcx protein sequences constitute the FCP of *T. lutea*, and at least five Fx molecules and nine Chl *a* and *c* molecules are bound to a majority of Lhcf monomers in this species [15]. In diatoms and haptophytes, a correlation was already established between the expression of the FCP and the concentration of pigments in cells. Especially, a clear correlation between the Lhcx and the photoprotective xanthophyll cycle Ddx-Dtx was observed in diatoms and haptophytes. In the diatom *Thalassiosira pseudonana*, both Dtx content and Lhcx proteins increased under high-light [9]. In *Phaeodactylum tricornutum*, the same correlation was observed between the Ddx-Dtx pool, three *lhcx* genes [10], and the Lhcx2 and Lhcx3 proteins [16,17]. In *T. lutea*, the

increase in Dtx was also correlated with the increase in *lhcx* genes expression under high light during a day:night cycle experiment [15].

Under high light conditions, Ddx and violaxanthin (Vx) are de-epoxidized into Dtx and Zx respectively. These reactions are driven by the diadinoxanthin de-epoxidase (DDE) and the violaxanthin de-epoxidase (VDE). Reverse reactions of epoxidation imply epoxidases, and take place at low light [18]. These enzymes are activated by the development of a light-driven proton gradient across the thylakoid membrane and an acidification of the thylakoid lumen [19]. Contrary to the Ddx-Dtx cycle, well-known and well-described in diatoms and haptophytes, the Vx-Zx cycle is usually associated to higher plants and green algae only [20–22]. However, this cycle is also present in brown algae, in diatoms, where it prevents photoinhibition [23,24], and haptophytes such as *T. lutea* as a secondary xanthophyll cycle [25,26]. Together with Lhcx proteins, both Ddx-Dtx and Vx-Zx cycles participate in the non-photochemical quenching (NPQ), more precisely the fast energy-dependent quenching (qE), which allows the dissipation, as heat, of excess excitation energy, induced by high irradiance [27]. In Chromista, models for NPQ measurement were established mainly for diatoms, and are not perfectly adapted to haptophytes, including *T. lutea* [28]. Indeed, the NPQ of *T. lutea* is sustained, which means NPQ is still present in darkness, *i.e.* its relaxation kinetics is not minutes but hours [29,30]. Therefore, the usual NPQ measure is not reliable for *T. lutea*. To overcome this problem, and in order to evaluate the dynamics between photochemistry and photoprotection, the measurement of the dark relaxation of the maximum quantum yield of the PSII (F_v/F_m) on steady-state photoacclimated microalgal cultures is required [29]. In these specific conditions, and as shown in diatoms, F_v/F_m is related to the NPQ extent and to the Dtx amount [29]

In this work, two clonal strains of *T. lutea* were selected for their different pigment composition. Indeed, it was previously observed that T-5cl6 accumulated more Dtx and Vx than T-4cl3, and that T-4cl3 produced 19 times more echinenone than T-5cl6 under N-deprivation condition (Pajot *et al.*, in prep.). The overall objective of this study was to understand how potentially different photoprotection strategies would be expressed in these two strains. Using turbidostat cultures, we examined in both strains the photoacclimative response (pigments and transcriptomics) and the extent of the dissipation of the excess light (dark F_v/F_m as a proxy for NPQ) as a function of increasing irradiance. The genes of interest we investigated were the genes coding for the light-harvesting antenna proteins (*lhcf*, *lhcx* and

lhcr), and for the de-epoxidases and epoxidases involved in the xanthophyll pigment cycles (DDE, VDE, ZE).

2. Materials and Methods

2.1. Culture conditions

Experiments were performed with two *Tisochrysis lutea* clonal strains, T-5cl6 and T-4cl3, respectively clone 6 from strain Ifremer-Argenton, isolated in Atlantic Ocean near Argenton, France and clone 3 from strain RCC1344, isolated in Atlantic Ocean at the level of the spanish coast. These strains were polyclonal and the different clones have been isolated by flow cytometry (platform Cytocell, University of Nantes, France). Current analyses performed in the laboratory are demonstrating genetic polymorphism between the two strains, resulted in phenotypic differences at the pigments and lipids content level.

We set up an experiment to observe the physiological response of the two strains with varying growth irradiances. Inoculum were maintained in Walne's medium (Walne, 1966) at 150 µmol photons m^{-2} s^{-1} (or PPF: Photosynthetic Photon Flux). The effect of different light irradiances (50, 150, 300 and 550 µmol photons m^{-2} s^{-1}) was determined for each strain in continuous 3.5 L photobioreactors (PBR). These PBR were made of two transparent polymethylmetacrylate (PMMA) columns (60 mm diameter) connected by two flanges (for design reference, see the single module in Loubière *et al.*, 2009 [31]). Light was delivered by six dimmable fluorescent white tubes. It was measured outside the PBR, at middle height between the two columns, using a spherical quantum sensor (LI-250 light meter, LI-COR, 3mm diameter).

Cultures were constantly aerated and thermoregulated at 26 ± 1°C by air conditioning and water circuit. pH was maintained constant at 8.2 with automatic injections of CO_2, measured with a pH measurement loop (electrode Inpro 4800/225/PT1000, Mettler Toledo and HPT 63, LTH electronics Ltd). Walne's medium enriched sea water (1 mL L^{-1}) was provided automatically by a metering pump (Simdos®) in order to maintain the culture at constant turbidity, *i.e.* at constant cell concentration. The excess culture was eliminated through an overflow pipe into a container. Cultures were monitored by a sensor to be maintained at low turbidity, between 1.5 and $2.5.10^6$ cells mL^{-1} (Fig. S4) in order to reduce self-shading and therefore keep the optical properties of the cultures stable. Each experiment was conducted in triplicate. Small error bars confirm the relevance of the three replicates in validating the

biological data (Fig. S4). Cultures were maintained seven to ten days at each light irradiance before sampling, in order for cells to acclimate and cultures to be at the equilibrium, *i.e.* at a steady-state. Cultures were assumed to be at steady-state when Chl *a* content was stable for at least three consecutive days with less than 10 % variation (Fig. S5, S6). In total, the experiment lasted four to five weeks per clonal strain.

2.2. Chl a*, cell concentration monitoring and growth rate*

To measure the Chl *a* content, cells were harvested daily from 10 mL of culture on a 0.2 µm fiberglass filter, and immediately immersed in 1.5 mL 95% acetone, during 24 hours. Absorbance was measured at 665 and 750 nm, before and after acidification with HCl 0.3 M. The number of cells per mL of culture (cell concentration, Fig. S4) was measured on a Multisizer Counter Coulter (Beckman Coulter®). Growth rate (µ) was measured daily by weighing the excess culture in the overflow container, which represented the daily dilution rate of the culture (Fig. S4).

2.3. Pigment extraction and HPLC analysis

Cell pigment content (Chl *a* in pg cell^{-1}, Fx, Ddx, Dtx and echinenone in mol(100 mol Chl *a*)$^{-1}$ was measured after seven to ten days at each light irradiance (50, 150, 300 and 550 PPF). Cells were harvested on a 0.2 µm fiberglass filter (GF/F, Whatman^{TM}) and immediately stored at -80°C. Four weeks later, they were immersed in 2 mL of 95% acetone, subjected to an ultrasonic bath for 10 minutes and placed at -20°C overnight. The acetone extracts were filtered on a 0.2 µm fiberglass filter prior to injection in HPLC. The filtered acetone extracts were analyzed by HPLC-UV-DAD (Agilent Technologies series 1200 HPLC-UV-DAD) using an Eclipse XDB-C8 reverse phase column (150 x 4.6 mm, 3.5 µm particle size, Agilent) following the method described by Van Heukelem & Thomas (2001) [32] with slight modifications. Briefly, solvent A was 70:30 MeOH: H_2O 28 mM ammonium acetate and solvent B was pure MeOH (Merck France). Gradient elution was the same as described in Van Heukelem & Thomas (2001) [32]. Quantification was carried out using external calibration against pigment standards (DHI, Denmark).

2.4. Chlorophyll fluorescence measurement

At steady-state, the triplicate culture subsamples acclimated to each growth irradiance were harvested. In parallel with pigment content, the chlorophyll fluorescence was measured with a PHYTO-PAM (WALZ). The effective PSII quantum yield in the dark (F_v/F_m) was measured

immediately after sampling, and following 15 min, 1 h and 2 h of dark acclimation, and calculated as:

$$F_v/F_m = \frac{F_m - F_0}{F_m}$$

With F0 and Fm the minimal and maximal fluorescence respectively.

2.5. RNAseq

At the steady-state, 50 mL of triplicate cultures acclimated to each growth irradiance were sampled for transcriptomic analysis. After centrifugation (10 min, 8000 g), total RNA was extracted from each strain (T-5cl6 and T-4cl3) using the TRIZOL reagent (Invitrogen, USA) according to the manufacturer's instructions. DNase treatment (DNase RQ1, Promega) was used to remove residual genomic DNA. The quantity of purified total RNA was determined by a Qubit 3 Fluorometer (Invitrogen, USA) using the AccuBlue® Broad Range RNA Quantitation Kit (Biotium, USA). The quality of purified total RNA was determined by measurement of absorbance (260 nm/280 nm) using a Nanodrop ND-1000 spectrophotometer (LabTech, USA). Poly(A) mRNA were selected, libraries of RNAseq were built using bare code according to Illumina's protocol. Sequencing was performed using the paired-ends method with an Illumina NovaSeq sequencer by the GenoToul platform (INRAE, Toulouse, France). The read length was 260 bases. Transcripts were normalized according to the median of ratio method proposed by the DESeq2 package in R: counts were divided by sample-specific size factors determined by the median ratio. The median ratio is the ratio of gene counts relative to geometric mean per gene. Table 1 shows the average number of normalized transcripts for each strain at each growth irradiance.

Table 1: Number of normalized reads for all growth irradiances for T-5cl6 and T-4cl3

	T-5cl6	T-4cl3
50 µmol $m^{2\ -1}$	3.3E+07	2.6E+07
150 µmol $m^2\ s^{-1}$	3.0E+07	2.5E+07
300 µmol $m^2\ s^{-1}$	3.2E+07	3.7E+07
550 µmol $m^2\ s^{-1}$	2.5E+07	2.8E+07

Raw reads of each sample were filtered using TrimGalore to remove known Illumina adapter sequences. Low quality reads were excluded using a quality score threshold of 30 and a minimal length of 75 or 150 bases. The quality of reads was assessed using FastQC. Then,

sequenced reads for each sample were aligned using HISAT2. Each gene within the alignment was counted using the Rsubread package in R with the function featureCounts, based on *T. lutea* reference genome [33]. Gene counts were obtained for each sample and normalized with DESeq2.

2.6. Similarity research

We performed a similarity research using BLAST [34] between the annotated DDE, VDE, VDL (violaxanthin de-epoxidase like) and VDR (violaxanthin de-epoxidase related) of several diatoms and haptophytes and *T. lutea* genome (Table S1, S2). All targets were selected and the best BLAST scores were selected as putative genes in *T. lutea*. For diatoms, there were one DDE from *Thalassiosira pseudonana*, nine VDE domain-containing proteins from *Fistulifera solaris*, *Thalassiosira oceanica* and *Thalassiosira pseudonana*, six VDE from *Fragilariopsis cylindrus*, *Phaeodactylum tricornutum*, *F. solaris*, two VDL precursors from *P. tricornutum*, two VDL from *T. pseudonana*, one VDR from *P. tricornutum*. For haptophytes, there were five VDE from *Chrysochromulina tobinii* and *Emiliania huxleyi*, four VDE domain-containing proteins from *E. huxleyi*, and one VDL from *C. tobinii*. We also considered the reverse reaction of epoxidation. We found several zeaxanthin epoxidases (ZE and ZE like: ZEL) but no diatoxanthin epoxidase was recorded in UniprotKB databases. In diatoms, there were nine ZE from *T. pseudonana*, *F. solaris*, *F. cylindrus*, *P. tricornutum* and one ZEL from *P. tricornutum*. In haptophytes, there were seven ZE from *C. tobinii* and *E. huxleyi*.

2.7. Statistics

For each average measure of the culture triplicates (pigment content and normalized transcript counts), we used a confidence interval, characterized by error bars on graphics, calculated at a 95% confidence level:

$$\text{Confidence interval} = Z_{a/2} * \frac{sd}{\sqrt{(n)}}$$

With $Z_{a/2} = 1{,}96,\ sd = \text{standard deviation}, n = 3$ (number of triplicates)

Statistical differences were calculated between T-5cl6 and T-4cl3. The p-values indicated in each figure is therefore representative of the difference between the two strains (except in Fig. 6). At each irradiance, the dataset was made of three values, corresponding to the three culture

replicates of T-5cl6 or T-4cl3. Therefore, a Student test was carried out first, and then an ANOVA test.

3. Results

3.1. Photosynthetic pigments and photochemical properties

Chl *a* content per cells gradually decreased with growth irradiance for both strains (Fig. 1A). In both strains, Fx normalized by Chl *a* gradually decreased with growth irradiance (Fig. 1B). At 50 PPF, T-5cl6 contained more Chl *a* than T-4cl3, and more Fx, as the Fx per Chl *a* ratio was similar in both strains. At 550 PPF it was the contrary, T-5cl6 contained less Chl *a* than T-4cl3.

In both strains, F_v/F_m decreased with the increase of growth irradiance (Fig. 1C). For all growth irradiances, F_v/F_m in T-5cl6 was lower than in T-4cl3. The difference between the two strains was the most significant at 150 PPF (pvalue < 0.01).

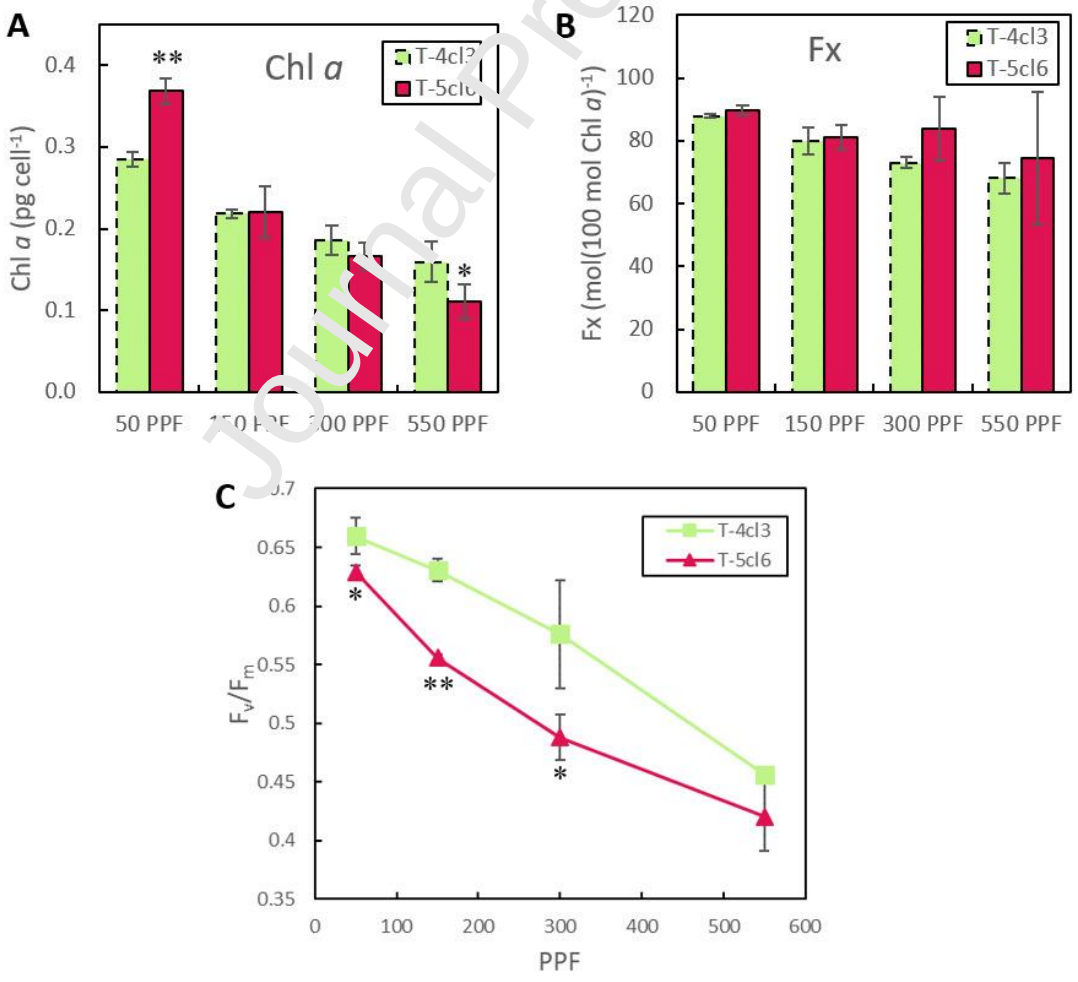

Figure 1: Evolution of the Chl *a* content (average ± the confidence interval, pg $cell^{-1}$) (A), of the Fx content normalized by Chl *a* (average ± the confidence interval, mol(100 mol Chl *a*)$^{-1}$) (B), of the maximum PSII quantum yield F_v/F_m (average ± the confidence interval) (C),relatively to growth irradiance (PPF = Photosynthetic Photon Flux = µmol m^2 s^{-1}). *: pvalue < 0.05, **: pvalue<0.01. *: pvalue < 0.05, **: pvalue<0.01.

3.2. Photoprotective pigments and F_v/F_m

With increasing growth irradiance, the Ddx+Dtx pool size increased 4-fold in T-5cl6 and 2.75-fold in T-4cl3 (Fig. 2A). The difference between the two strains was mainly explained by the highly variable values of Dtx amount (Fig. 2B) which increased 30.5-fold in T-5cl6 and 25.5-fold in T-4cl3 between 50 and 550 PPF. Furthermore, at 50, 150, 300 and 550 PPF, there was respectively 2, 4, 3 and 2.5 more Dtx in T-5cl6 than in T-4cl3. In parallel, the de-epoxidation state of Ddx to Dtx (DES-DD), expressing the conversion of Ddx into Dtx as a photoprotection mechanism, was calculated (Fig. 2C). At the lowest irradiance of 50 PPF, the DES-DD was 4% for T-4cl3 and significantly higher for T-5cl6, 9%. For both strains the DES-DD increased with increasing growth irradiance, and values were higher for T-5cl6 at all four growth irradiances. At the highest irradiance, 550 PPF, the DES-DD reached 66% for T-5cl6 and 40% for T-4cl3 (Fig. 2C).

The maximum PSII quantum yield (F_v/F_m) was expressed as a function of the normalized amount of Dtx to Chl *a* (Fig. 2D). Trend lines of both strains have a $R^2 > 0.97$, which demonstrated a solid correlation between F_v/F_m and Dtx (Fig. 5D). The slope of the T-4cl3 trend line was higher than the one of T-5cl6.

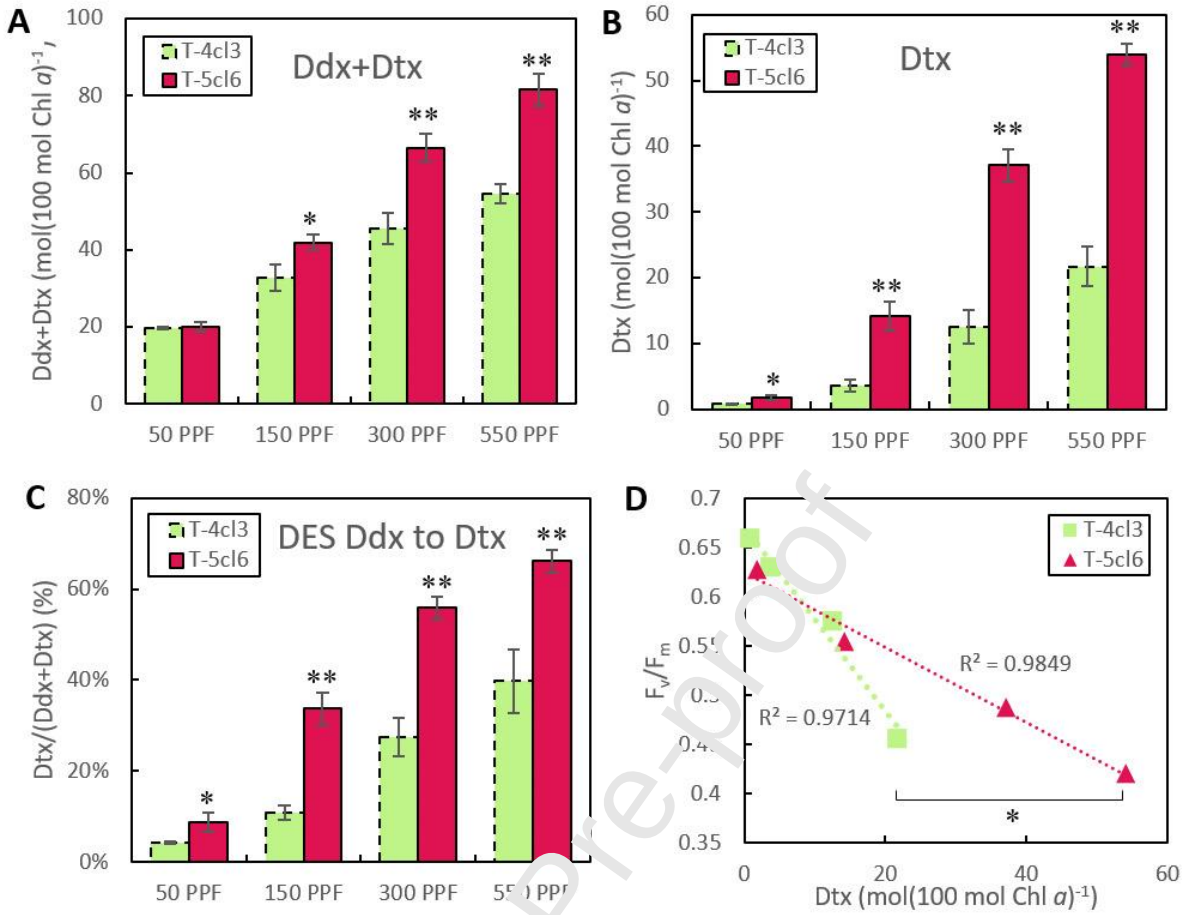

Figure 2: Evolution of the Ddx+Dtx pool (A) and of the Dtx (B) normalized by Chl *a* (average ± the confidence interval, mol(100 mol Chl *a*)$^{-1}$), of the de-epoxidation state (DES) from Ddx into Dtx (C) relatively to growth irradiance (PPF = Photosynthetic Photon Flux = µmol m^2 s^{-1}). (D) presents the F_v/F_m relatively to Dtx content and the significant difference between the two slopes. *: pvalue < 0.05, **: pvalue < 0.01.

The Vx+Zx pool size increased with increasing growth irradiance, and values for T-5cl6 were significantly higher than for T-4cl3 (Fig. 3A). As for Dtx, Zx was significantly higher in T-5cl6 from 150 to 550 PPF than in T-4cl3 where Zx was synthetized in small amounts at 550 PPF only (Fig. 3B). Values of the de-epoxidation state from Vx to Zx (DES-VZ) showed that in T-5cl6, Vx was converted into Zx gradually with increasing growth irradiance, and reached 50% at 550 PPF (Fig. 3C). In T-4cl3, only 9% of Vx was converted into Zx at 550 PPF. F_v/F_m was expressed relatively to the photoprotective pigment Zx (Fig. 3D). The slope of T-4cl3 was higher than the one of T-5cl6, it was associated with 6.5-fold less Zx than in T-5cl6.

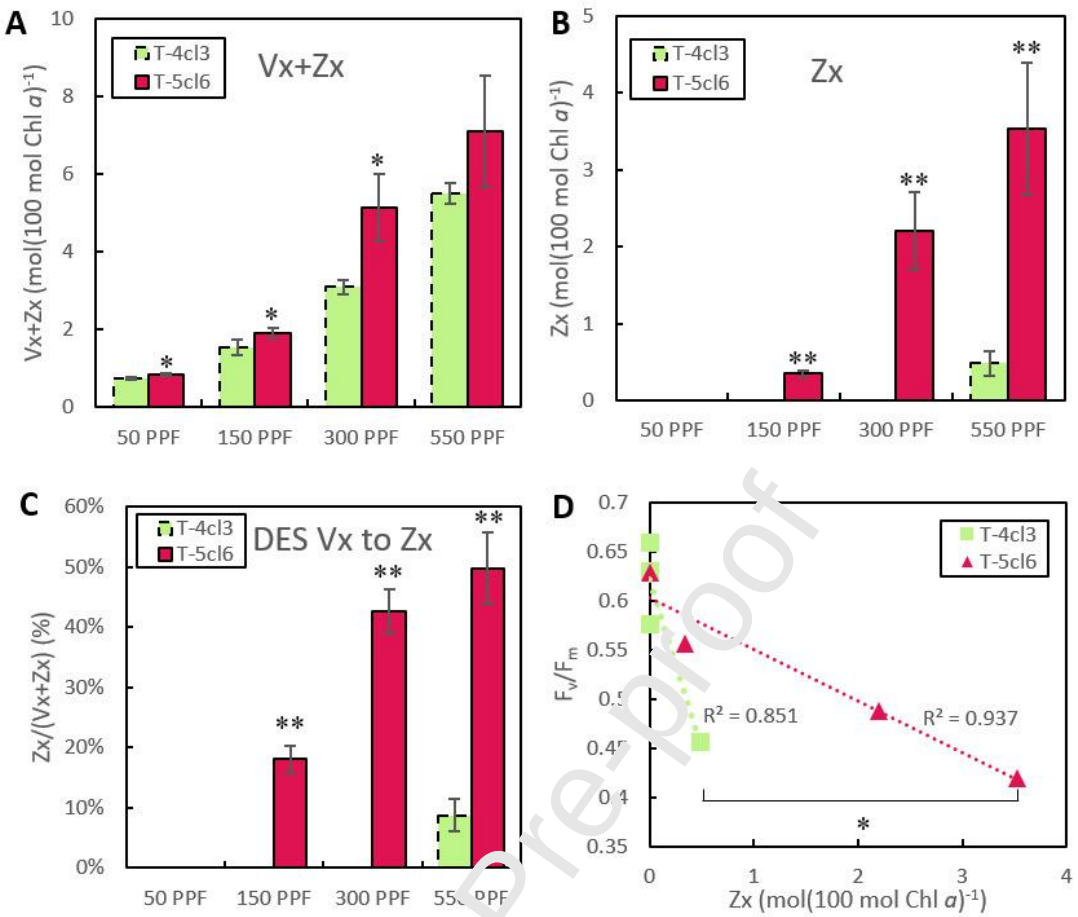

Figure 3: Evolution of the Vx+Zx pool (A) and of the Zx (B) normalized by Chl *a* (average ± the confidence interval, mol(100 mol Chl *a*)$^{-1}$), of the de-epoxidation state from Vx into Zx (C) relatively to growth irradiance (PPF = Photosynthetic Photon Flux = µmol m^2 s^{-1}). (D) presents the F_v/F_m relatively to Zx content and the significant difference between the two slopes. *: pvalue < 0.05, **: pvalue < 0.01.

In our growth conditions, the pigment echinenone was found only in T-4cl3 strain at 300 PPF and 550 PPF, and was increasing with growth irradiance (Fig. 4). At 550 PPF, echinenone represents 17% of the total carotenoids in T-4cl3 and 24% of the Chl *a* amount.

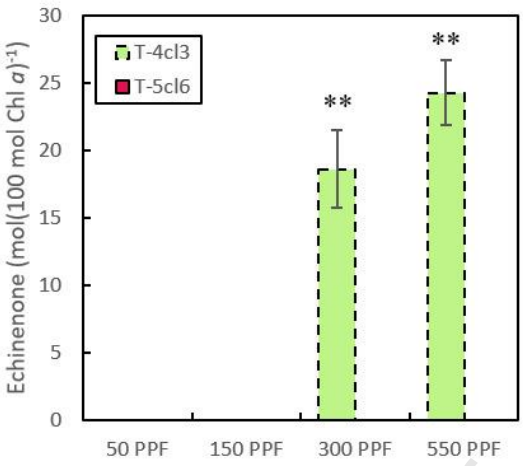

Figure 4: Evolution of the echinenone normalized by Chl *a* (average ± the confidence interval, mol(100 mol Chl *a*)$^{-1}$) relatively to growth irradiance (PPF = Photosynthetic Photon Flux = µmol m^2 s^{-1}). **: pvalue < 0.01.

In order to observe the dynamic balance between photosynthesis and photoprotection, we measured the F_v/F_m and the pigment content of cultures after 0 min, 15 min, 1 hour and 2 hours of darkness for each growth irradiance (Fig. 5A). For all conditions, F_v/F_m was lower in T-5cl6 than in T-4cl3. For all growth irradiances, F_v/F_m strongly increased after 20 min of darkness and kept increasing after 60 and 120 min. In parallel, Dtx content gradually decreased while Ddx content gradually increased as Dtx was re-epoxidized into Ddx (Fig. 5B, 5C). Both pigments were higher in T-5cl6 than in T-4cl3. At 550 and 300 PPF, Ddx and Dtx contents respectively doubled and halved after 120 min of darkness in T-5cl6. Proportions were lower in T-4cl3. After 120 min of darkness, there was still Dtx left in the culture samples of both strains which increased with growth irradiance.

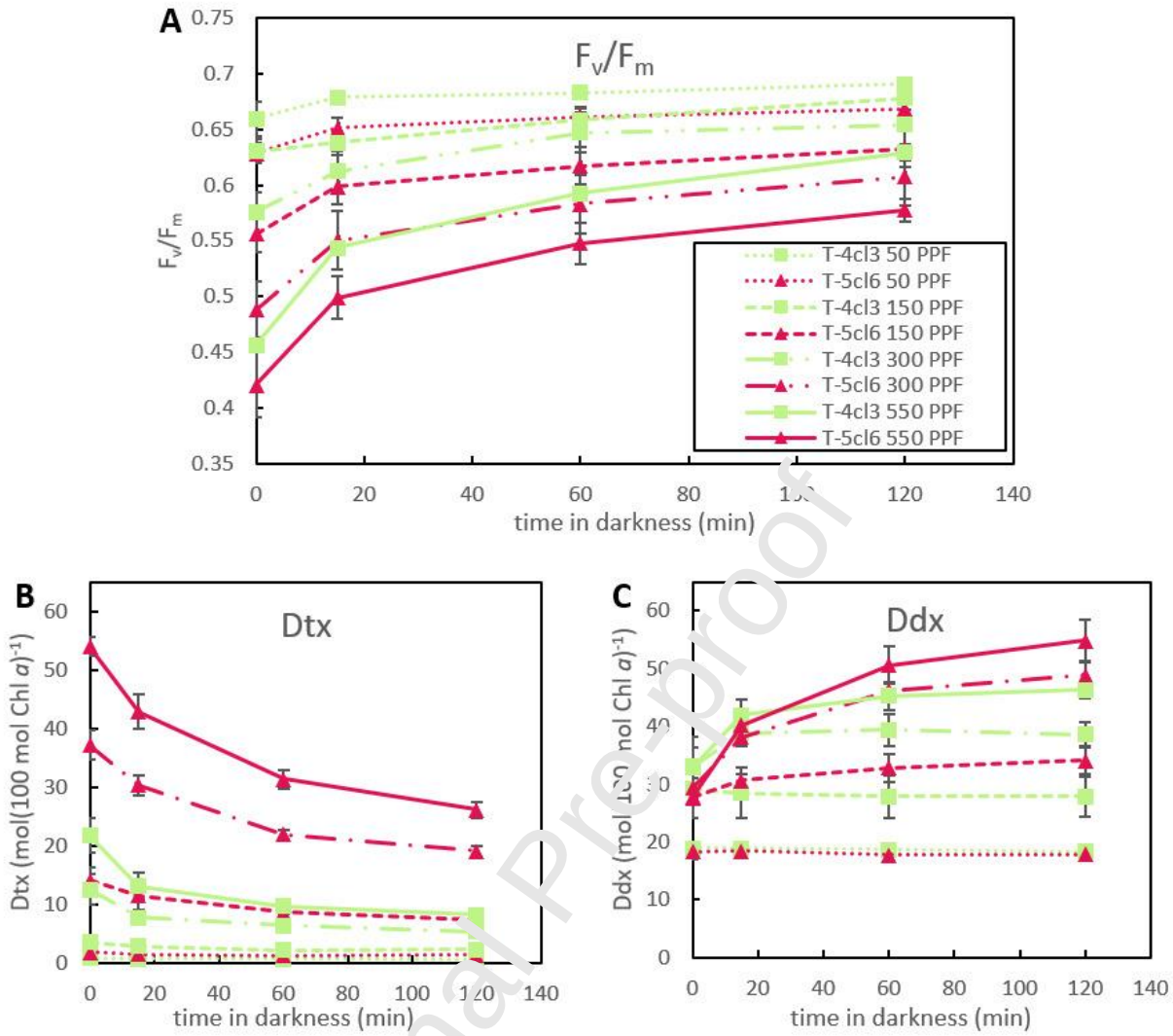

Figure 5: Evolution of F_v/F_m (A), of Dtx content (B) and of Ddx content (C) normalized by Chl *a* (average ± the confidence interval, mol(100 mol Chl *a*)$^{-1}$) relatively to the time in darkness.

3.3. Expression of lhc genes

We observed the evolution of the *lhcx* expression in both strains under the four growth irradiances (Fig. 6, Fig. S1). The heatmap in Fig. 6 shows the expression level of *lhcx* genes and the significant difference between the four growth irradiances for both strains. Transcripts amounts of *lhcx2* were by far the highest especially at 50 PPF in T-4cl3, followed by *lhcx1* transcripts accounts. In T-4cl3, 8 *lhcx* upon 12 were remarkably and significantly upregulated at 150 PPF (*lhcx1*, *lhcx3*, *lhcx4*, *lhcx8*, *lhcx9*, *lhcx10*, *lhcx11*, *lhcx12*).

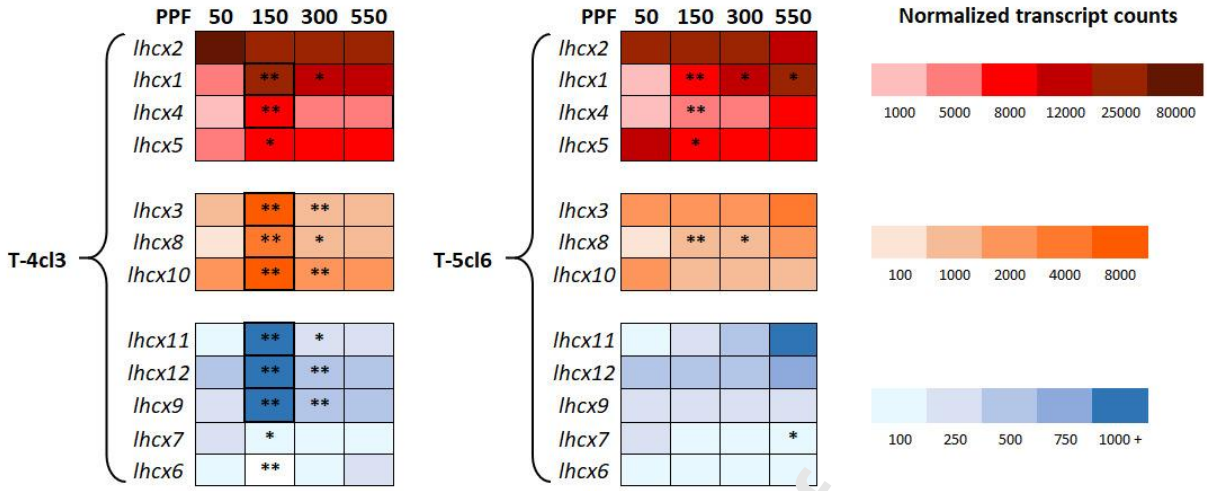

Figure 6: Heatmap of the *lhcx* transcripts counts. *: pvalue < 0.05, **: pvalue < 0.01. Thick borders correspond to the highly upregulated *lhcx* genes at 150 PPF in T-4cl3.

Overlooking the upregulation at 150 PPF, *lhcx1*, *lhcx3*, *lhcx4*, *lhcx8* and *lhcx11* were gradually upregulated with increasing growth irradiance in both strains, up to five to ten-fold. At the highest growth irradiance (550 PPF), these genes were more expressed in T-5cl6 than in T-4cl3. In T-4cl3, *lhcx2* and *lhcx6* were upregulated at 50 PPF and *lhcx5* was downregulated at 50 PPF. On the contrary, *lhcx2*, *lhcx5* and *lhcx7* were gradually downregulated with increasing growth irradiance in T-5cl6.

In T-4cl3 among the 12 *lhcr*, 10 were downregulated from 150 PPF to 550 PPF (Fig. S2), their expression was minimum at 50 PPF (Fig. S2). In T-5cl6, a similar pattern was observed, 10 *lhcr* were downregulated with increasing growth irradiance from 50 to 550 PPF (all but *lhcr5* and *lhcr6*) (Fig. S2). In T-4cl3, *lhcr5* and *lhcr6* were upregulated only under 150 PPF (Fig. S2), like the majority of *lhcx* (Fig. 6), while in T-5cl6 they were upregulated with increasing growth irradiance. None of the *lhcf* genes were remarkably upregulated at 150 PPF (Fig. S3). In T-4cl3, the decreasing pattern with increasing growth irradiance from 50 to 550 PPF was only obvious for *lhcf13*, *lhcf21*, *lhcf24*, *lhcf26* and *lhcf27*. In T-5cl6, all 28 *lhcf* were downregulated with increasing growth irradiance (Fig. S3). The expression of other genes in T-4cl3 was either relatively stable without significant variations, either slightly decreased from 150 PPF to 300 and 550 PPF. Indeed, in T-4cl3, 15 *lhcf* among 28 were the least expressed at 50 PPF compared with other irradiances (*lhcf1*, *lhcf2*, *lhcf3*, *lhcf4*, *lhcf5*, *lhcf6*, *lhcf7*, *lhcf8*, *lhcf17*, *lhcf18*, *lhcf19*, *lhcf20*, *lhcf22*, *lhcf25*, *lhcf28*). At 50 PPF, except for *lhcf22*

and *lhcf23*, all *lhcf* were more expressed in T-5cl6 than in T-4cl3. Under the other growth irradiances, almost half of *lhcf* (12 among 28) were more expressed in T-5cl6 than in T-4cl3.

3.4. Expression of de-epoxidase and epoxidase genes

3.4.1. Diadinoxanthin de-epoxidase, DDE

The similarity research with the DDE of *T. pseudonana* as a query resulted in four *T. lutea* genes, with the best similarity score for TISO_37047 (259) (Table S1). Furthermore, TISO_37047 had lower similarity scores with all other VDE, VDL (violaxanthin de-epoxidase like) or VDR (violaxanthin de-epoxidase related) of diatoms than with the DDE of *T. pseudonana*, although it had higher scores with a VDE domain-containing protein of the haptophyte *E. huxleyi*. Considering the fact that no DDE was annotated yet for haptophytes, and that VDE and DDE domains might resemble, TISO_37047 was the best candidate as a putative DDE enzyme. We decided to annotate this gene as DDE_L (DDE_like) in *T. lutea*. According to the Interproscan analysis of this sequence, DDE_L possesses several VDE domains (Table S5). We noticed that in all Interproscan database, there was no DDE domain referenced. We monitored the evolution of DDE_L expression as a function of growth irradiance (Fig. 7). DDE_L expression in T-5cl6 was higher than in T-4cl3 under all four growth irradiances, and significantly at 50, 300 and 550 PPF. At 50 and 550 PPF, DDE_L was 3.5 times more expressed in T-5cl6 (p-value < 0.01), and transcripts accounts at these two irradiances were similar in both strains respectively. More generally, in T-5cl6, DDE_L expression increased gradually from 150 to 550 PPF while in T-4cl3 transcripts accounts were similar at 50, 300 and 550 PPF and maximum at 150 PPF (Fig. 7). No Dtx-epoxidase were found in the UniprotKB database.

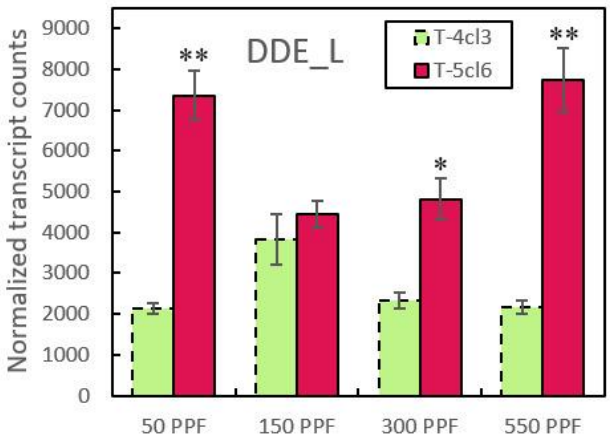

Figure 7: Evolution of normalized transcript counts of DDE_L (average ± the confidence interval) relatively to growth irradiance (PPF = Photosynthetic Photon Flux = µmol m^2 s^{-1}). *: pvalue < 0.05, **: pvalue < 0.01.

3.4.2. Violaxanthin de-epoxidase, VDE and zeaxanthin epoxidase, ZE

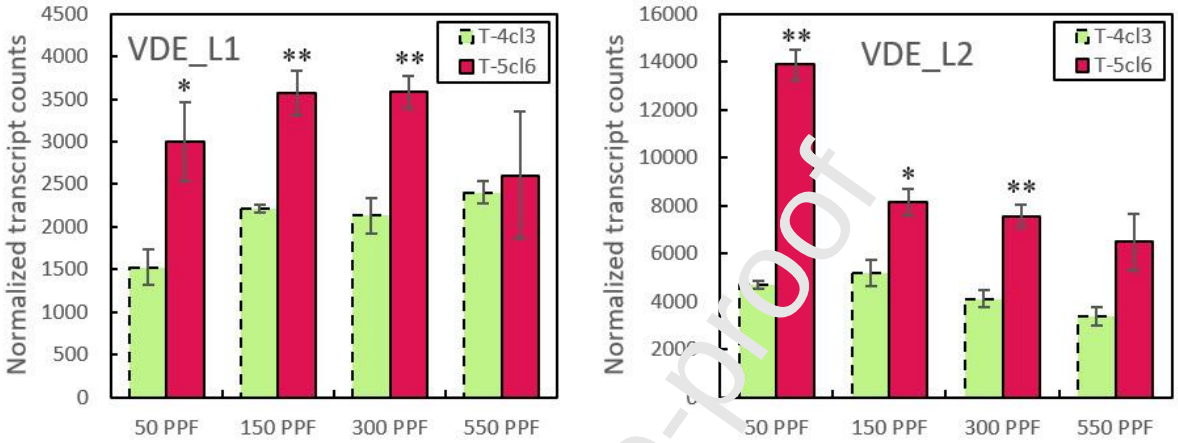

Figure 8: Evolution of TISO_01606 (VDE_L1) and TISO_02731 (VDE_L2) normalized transcripts counts (average ± the confidence interval) relatively to growth irradiance (PPF = Photosynthetic Photon Flux = µmol m^2 s^{-1}). *: pvalue < 0.05, **: pvalue < 0.01.

The similarity research with the VDE, VDL and VDR of diatoms and haptophytes as a query resulted in five *T. lutea* genes. The same five genes were found throughout the similarity research with diatoms and the one with haptophytes. According to Interproscan analysis of the molecular function, all five genes possess a VDE activity (Table S5). The best similarity scores were obtained with haptophyte sequences. TISO_01606 especially obtained the highest similarity score of all sequences, with the VDE2 sequence of *E. huxleyi* (600, Table S2). TISO_01606 was named VDE_L1 (VDE_Like1) and considered as coding for a putative VDE enzyme. The alignment of VDE_L1 of *T. lutea* and VDE2 of *E. huxleyi* resulted in 67.4% similarity. Interestingly, VDE_L1 expression was significantly higher in T-5cl6 than in T-4cl3 at 50, 150 and 300 PPF but not at 550 PPF (Fig. 8). In T-5cl6, VDE_L1 increased from 50 to 150 PPF then stabilized at 300 PPF and decreased at 550 PPF. TISO_02731 showed high similarity score with the VDE of *C. tobinii* and a VDE domain-containing protein of *E. huxleyi* (respectively 418 and 400) (Table S2), and as such was considered as coding for a putative VDE enzyme. TISO_02731 was named VDE_L2 (for VDE_Like2). VDE_L2 expression was higher in T-5cl6 than in T-4cl3 under all growth irradiances, and

significantly at 50, 150 and 300 PPF (Fig. 8). In both strains, but especially in T-5cl6, its expression decreased with increasing irradiance. According to Interproscan analysis (Table S5), VDE_L2 was associated with two biological processes, potassium ion transport and transmembrane transport, and two molecular functions, voltage-gated potassium channel activity and VDE activity. VDE_L2 was the only gene which was not exclusively associated to VDE activity among the five genes found with the similarity research.

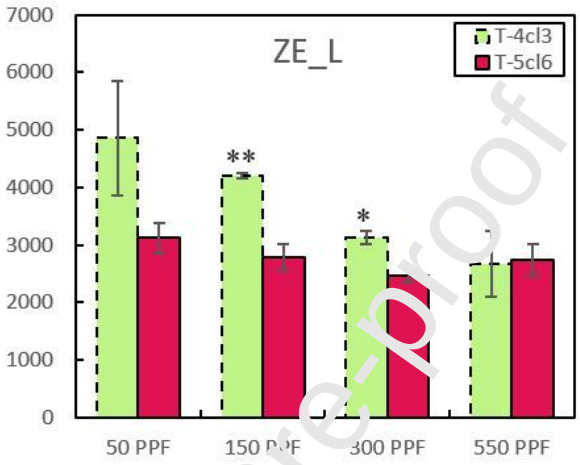

Figure 9: Evolution of TISO_33049 (ZE_L) normalized transcripts counts (average ± the confidence interval) relatively to growth irradiance (PPF = Photosynthetic Photon Flux = µmol m^2 s^{-1}). *: pvalue < 0.05, **: pvalue < 0.01.

The similarity research with the ZE of diatoms and haptophytes as a query resulted in eleven *T. lutea* genes (Table S3, S4). Among them, TISO_30349 had the highest similarity score with a ZE in *E. huxlevi* (678) (Table S4). TISO_30349 was therefore considered as coding for a putative ZE enzyme and named ZE_L (for ZE_Like). With increasing growth irradiance, the expression of ZE_L decreased in both strains (Fig. 9). At 150 and 300 PPF, ZE_L was significantly more expressed in T-4cl3.

4. Discussion

4.1. Different photoprotection strategies in T. lutea *T-5cl6 and T-4cl3 strains*

4.1.1. The Ddx-Dtx and Vx-Zx xanthophyll cycles

As cells maintained growth efficiency under light stress, as shown with the increasing growth rate in Fig. S4, the observed molecular events such as photoprotective pigments synthesis really protected the cells from damage. The two *T. lutea* clonal strains, T-5cl6 and T-4cl3, were grown in the exact same conditions of irradiance, temperature, pH, nutrients, and at the

same cell concentration. The ratio of Fx/Chl *a* was lower in T-4cl3 than in T-5cl6, suggesting that the light-harvesting capacity under high light was lower in T-4cl3. Using the darkness relaxation of F_v/F_m as a proxy for NPQ [29], we monitored a strong correlation with the Dtx content, pointing out to an implication of Dtx in the photoprotective dissipation of excess light energy in both strains. The decrease of photochemistry in T-4cl3 was associated to 2.5-fold less amount of Dtx than in T-5cl6, suggesting differences in quenching efficiency of Dtx between the two strains. Moreover, as in diatoms, Ddx was not entirely de-epoxidized in Dtx (*i.e.* maximum DES was about 60%), highlighting the double role of Ddx as a photosynthetic pigment and as a precursor of Dtx [35]. The same hold true for the photoprotective couple pigment Vx and Zx, as previously reported in diatoms [36]. In T-5cl6, photoprotection was associated with a higher Dtx and Zx content than in T-4cl3, with Zx only accumulated at 550 PPF in T-4cl3. Instead, T-4cl3 produced echinenone at 300 and 550 PPF while T-5cl6 did not. In summary, T-5cl6 used the two xanthophyll cycles Ddx-Dtx and Vx-Zx, and associated NPQ, as major photoprotective mechanisms, similarly as in diatoms [16]. Both cycles were used to a lower extent and more sequentially by T-4cl3. In addition, T-4cl3 cells strengthened their photoprotective pigment panel by producing echinenone at a certain threshold between 150 and 300 PPF. At 550 PPF, Dtx and echinenone were probably not sufficient to endorse the excess light energy in T-4cl3 cells and they started de-epoxidizing Vx into Zx. It is likely that at higher irradiances above 550 PPF, the Zx and echinenone concentrations would increase even more.

4.1.2. The remarkable presence of echinenone in T-4cl3

The most noteworthy result of this study was the appearance of echinenone in T-4cl3 cells at 300 PPF. The presence of echinenone was previously demonstrated in *T. lutea* strain CCAP 927/14 [37] and in a close species, *Isochrysis galbana*, under N-deprivation [37,38]. In addition, we observed that T-4cl3 also synthetized echinenone under N-deprivation (Pajot *et al.* in prep). In *T. lutea* strain CCAP 927/14, it was reported that echinenone represented 25% of total carotenoids under N-deprivation [37]. Our results showed that echinenone represented a similar high amount of 17% of total carotenoids under N-replete condition at high irradiance. Echinenone is usually found in cyanobacteria, it scavenges the ROS [39] under high irradiance, and as such participates to photoprotection. In cyanobacteria, under high irradiance, the thermal dissipation of the light energy absorbed in excess by the phycobilisome (the light-harvesting antenna of cyanobacteria) is also mediated by a NPQ mechanism, which regulatory partners are different from haptophytes and diatoms [40].

Cyanobacteria NPQ occurs when the echinenone is bound to the Orange Carotenoid Protein (OCP) [41,42]. For instance, in *Synechocystis sp.*, NPQ is only activated when the 3′-hydroxyechinenone is bound to the OCP [43]. Our work is a first report of the presence of echinenone in a haptophyte under high light. According to several similarity researches we performed, no OCP was found in *T. lutea*. However, our results support that in the strain T-4cl3, the echinenone played a role in the response to high light as a support to the xanthophyll cycles-mediated NPQ, likely through direct ROS scavenging [44], *i.e.* by free-echinenone molecules in the thylakoid membrane, similarly as some Dtx molecules [45]. Nevertheless, we cannot exclude that a different form of the OCP is present in *T. lutea*, and further search is required.

4.2. Xanthophyll de-epoxidases and epoxidases in T. lutea

This is the first time that several DDE and VDE candidate genes were characterized in *T. lutea*. The monitoring of their expression as a function of growth irradiance enabled to correlate the transcription of these genes to the different light-response strategies shown by T-5cl6 and T-4cl3. No Dtx-epoxidase was found in the UniprotKB database. However, the two Dtx-epoxidases of *Thalassiosira pseudonana* are usually annotated as ZE in the literature [46]. Therefore, the seven sequences in *T. lutea* resulting from the research similarity with the query sequence "ZE Thalassiosira pseudonana THAPSDRAFT 261390" (Table S3) might be good candidates as Dtx-epoxidase.

As pointed out before in the diatom *P. tricornutum*, the zeaxanthin-epoxidase (ZE) can play an equivalent role, i.e. ZE can trigger the epoxidation of both Dtx and Zx [30,43].

4.2.1. The diadinoxanthin de-epoxidase

With increasing growth irradiance, Ddx was de-epoxidized into Dtx as illustrated by the progressive increase in DES-DD in both strains. Ddx de-epoxidation was stronger in T-5cl6 than in T-4cl3. We found a DDE gene candidate we named DDE_L, whose associated protein could be responsible of the Ddx de-epoxidation in *T. lutea*. As for Dtx content and DES-DD, DDE_L expression was higher in T-5cl6 than in T-4cl3 under all four irradiances, which was consistent with a stronger Ddx de-epoxidation activity in T-5cl6. Interestingly, in T-5cl6, the expression of DDE_L was close to its maximum already at 50 PPF. In parallel, we did not observe a particular Dtx accumulation that could have been induced by chlororespiratory electron flow, as it was reported in the diatom *Phaeodactylum tricornutum* [48]. This result

might suggest that T-5cl6 cells produce a maximum of DDE_L transcripts regardless of the irradiance, without translating them into protein unless it is necessary. Or, the associated protein of DDE_L has a more complex role than the putative de-epoxidation of Ddx. In *P. tricornutum*, the inactivation of the DDE enzyme under low light was shown not to be the factor triggering the inactivation of Dtx synthesis and NPQ maintenance [47]. Instead, they were due to an increase in Dtx epoxidation, which was therefore proposed to be the main actor in the Ddx-Dtx xanthophyll cycle regulation.

4.2.2. The violaxanthin de-epoxidase and the zeaxanthin epoxidase

The difference between the two clonal strains was also witnessed by the expression level of the Vx-Zx cycle associated genes. Among them, the expression of TISO_01606, we named VDE_L1, was significantly higher in T-5cl6 at almost all growth irradiances, and it increased with increasing growth irradiance. A second putative candidate, TISO_02731, we named VDE_L2, was found to be associated to both a VDE activity and a voltage-gated potassium channel protein. A voltage-gated potassium channel protein is a complex forming a transmembrane channel through which potassium ions may cross a cell membrane in response to changes in membrane potential [49]. It is noteworthy that VDE_L2 could regulate in parallel both the de-epoxidation of Vx and the pH lumen which is itself pH-dependent [20,50]. Such potential dual role would need further investigation, ideally with targeted knock-out mutagenesis, as in diatoms [51]. Furthermore, VDE_L1 in *T. lutea* had the best similarity score with the VDL2 gene of *P. tricornutum* (gene identification: PHATRDRAFT_45846), which encodes for an enzyme that has recently been demonstrated to be central in the Fx biosynthetic pathway in a study by Bai *et al.* (2022) [52]. This study suggested that Ddx would also be a substrate for the VDL2 enzyme, in addition to Vx. VDL2 would indeed be able to catalyze the tautomerization reaction (isomerization of a molecular function) of Ddx to allenoxanthin, these two pigments being key precursors of the Fx synthesis [52]. In addition, it is specified that the VDL2 enzyme in *P. tricornutum* is most likely subject to strict regulation in diatoms and haptophytes, so that Ddx can play both its role as a precursor of the major photosynthetic pigment that is Fx, and its role in photoprotection within the Ddx-Dtx cycle.

In the diatom *P. tricornutum*, NPQ results from the early inhibition of ZE rather than from an activation of DDE/VDE, which increases the amount of Dtx and, under certain light conditions, of Zx [47].The epoxidation is the reverse reaction of the Ddx-Dtx and Vx-Zx

cycles and it usually corresponds to a decrease in light intensity. In *T. lutea*, ZE_L gene seems to be a strong candidate to code for a zeaxanthin epoxidase. In both strains, the ZE-L transcript level was similar to the ones of DDE and VDE, it was the highest at 50PPF, and its expression decreased with increasing growth irradiance, and might correspond to a lower synthesis of the ZE_L associated protein. This pattern is usual and might be interpreted as the need of cells for keeping the right balance between light-harvesting (Ddx and Vx) and photoprotective (Dtx and Zx) pigments as a function of the growth irradiance. In the study by Bai *et al.*, (2022) [52], the ZEP1 (zeaxanthin epoxidase) gene in *P. tricornutum* (gene identification: PHATRDRAFT_45845) has been shown, as VDL2, to code for a central enzyme in the Fx biosynthetic pathway [52]. Since ZE_L in *T. lutea* had a high similarity score with ZEP1, it is assumed that its role, in addition to the epoxidation of Zx, is also central in the biosynthesis of Fx in *T. lutea* and in haptophytes in general.

4.3. A sustained NPQ in T. lutea

Culture samples were exposed to darkness in order to observe the relaxation dynamics from photoprotection back to photochemistry. Surprisingly, after two hours of darkness exposure, there was still Dtx present in cells of both strains, indicating that the epoxidation reaction from Dtx to Ddx was not complete. It has been determined that in algae using the Ddx-Dtx cycle as a photoprotective mechanism, the switch of the light-harvesting antenna from the NPQ mode to the light-harvesting mode at lower irradiance can only be realized by an efficient removal of Dtx [53]. Nevertheless, under some harsh conditions (very high light, low temperature), the presence of Dtx, even after prolonged darkness, *i.e.* several hours and days, can be 'constitutive' and can generate a sustained form of NPQ [28,29]. This form of NPQ is complementary to the main NPQ component, qE [28,46,54], which is usually turned off in a few tens of seconds to some minutes when the cells are transferred from excess light to lower light or darkness [10]. In *T. lutea*, the retention of Dtx under prolonged darkness was especially strong in T-5cl6 under the highest irradiances. It was correlated with a partial relaxation on F_v/F_m likely illustrating a strong sustained NPQ [29]. It is noteworthy that T-5cl6 is the strain which relies the most on xanthophyll cycles. A stronger sustained NPQ is likely to be part of its photoprotective strategy, allowing the cells to promptly respond to an anticipated increase in irradiance after the darkness period [29].

4.4.The role of lhcx in T. lutea

4.4.1. lhcx1, lhcx4, lhcx8 and lhcx11 as major actors in regulating NPQ?

The increase of photoprotective pigments such as Dtx and Zx does not necessarily lead to higher effective NPQ. Indeed in diatoms, it is the binding of photoprotective pigments to Lhc proteins, especially Lhcx, that effectively involves these pigments in NPQ [10]. Dtx molecules can be freely present in the thylakoid membrane to directly scavenge ROS species [45]. In both *T. lutea* strains, *lhcx1*, *lhcx4*, *lhcx8* and *lhcx11* were gradually upregulated with increasing growth irradiance together with Dtx synthesis. It suggests that *lhcx1*, *lhcx4*, *lhcx8* and *lhcx11* could be Dtx binders and potentially major actors in regulating NPQ in *T. lutea*. Interestingly, the transcript level of these genes was not particularly different between both strains (but for 150 PPF, see below) although NPQ was significantly stronger in T-5cl6, with the only exception of *lhcx11* at 550 PPF for which there was no difference in NPQ. Therefore, the NPQ difference can only be explained by the highest transcription of *lhcx* genes in corresponding proteins in T-5cl6 for providing the necessary binding sites to the significantly higher amount of Dtx molecules in this strain. Western-blot analysis will be needed to further confirm this hypothesis [17,55]. Besides *lhcx*, two *lhcr* genes, *lhcr5* and *lhcr6*, were upregulated with increasing growth irradiance in both strains. Interestingly, *lhcr5* and *lhcr6* form, together with *lhcr10*, a subclade of the *lhcr* family in *T. lutea* [15]. Moreover, *lhcr5* and *lhcr6* are similar to *lhcr6* and *lhcr8* in *P. tricornutum*, which were proposed to play a role in photoprotection [15,56]. It is therefore consistent that *lhcr5* and *lhcr6* were expressed similarly to the majority of *lhcx* in T-4cl3. This result confirmed their supposed function in photoprotection, and possibly in NPQ.

4.4.2. lhcx2 and lhcx5 prevent an increase in irradiance?

Among *lhcx* genes, *lhcx2*, *lhcx5* and *lhcx7* were the only genes downregulated with increasing growth irradiance. In particular, *lhcx2* was highly expressed at 50 PPF in T-4cl3. Similarly, in our previous study on *T. lutea* strain CCAP 927/14, *lhcx2* was the only gene upregulated at low light, and during the night [15]. The hypothesis was that the associated Lhcx2 protein could protect from the return of light at any time after prolonged darkness exposure, as proposed for Lhcx4 in the diatom *P. tricornutum* [57]. The function of *lhcx2* in *T. lutea* strain CCAP 927/14 and T-4cl3 might therefore be extended to respond to a potential increase of irradiance during a low light period acclimation. In T-5cl6, this role might be undertaken by *lhcx5* which was also highly expressed at 50 PPF compared with T-4cl3. Transcript accounts of *lhcx2* and *lhcx5*, as well as the high light upregulated *lhcx1* and *lhcx4*, were the highest in both strains. Thus, corresponding proteins, if translation would be paralleled, might play an

important role in light-response and possibly be predominant in the structure of the FCP in *T. lutea*.

4.4.3. lhcx participate in the balance between photochemistry and photoprotection?

We observed a significant spike of expression for eight *lhcx* and two *lhcr* (*lhcr5* and *lhcr6*) at 150 PPF in T-4cl3. It was not paralleled with photoprotective pigments. The increase of *lhcx* and *lhcr* expression at 150 PPF was therefore not considered as inherent to photoprotection mechanisms under to the highest irradiances. In a previous experiment, the same 8 *lhcx* of *T. lutea* strain CCAP 927/14, cultivated with a day:night cycle, were significantly upregulated at the beginning of the day, corresponding to 225 PPF, compared to midday, corresponding to 900 PPF [15]. The hypothesis was that cells overexpressed *lhcx* at the beginning of the day to endorse light onset without risking photodamage. With our results in this work, the explanation could finally be different. We hypothesize that 150 PPF is a threshold between photochemistry and photoprotection for T-4cl3, *i.e.* that 150 PPF would be close to E_K, the light saturation parameter for growth. This possibility is supported by the sharper decrease in F_v/F_m beyond 150 PPF in T-4cl3. Another possibly, not exclusive, and depending on transcript translation, is the need for specific Lhcx and/or Lhcr FCP subunits in the light-harvesting antenna, in order to perform the best adjustment between photochemistry and photoprotection at 150 PPF and beyond.

5. Conclusion

This study investigated the differences of photoprotection strategies between two clonal strains of the haptophyte *Tisochrysis lutea*. Overall, our results showed that with increasing growth irradiance, the expression of the *lhcx* genes increased and it was correlated with a gradual increase of the content in photoprotective pigments and of the dissipation of light energy in excess. Both strains differed with their photoprotective pigment (Table 2). T-5cl6 strain strategy was predominantly based on the Ddx-Dtx and the Vx-Zx xanthophyll cycles, while T-4cl3 strain strategy was also based on the Ddx-Dtx cycle, but to a lesser extent, and on the parallel echinenone accumulation. At higher irradiances, when both Dtx and echinenone appeared to be insufficient to endorse the excess light energy, the photoprotective pigment content was completed with the Vx-Zx cycle.

In both strains, the fine balance between photosynthesis and photoprotection was performed by the combination of (Table 2) (1) the FCP structuration with *lhcx*, *lhcr* and *lhcf*, (2) the

modulation of the photosynthetic pigments chlorophylls and fucoxanthin, (3) the synthesis of photoprotective pigments of the Ddx-Dtx and the Vx-Zx xanthophyll cycles, alongside with the transcription of de-epoxidases and epoxidases, and of the echinenone in T-4cl3 specifically. The differences between the two clonal strains highlighted precise correlations between these regulatory partners. We propose these differences are likely due to their adaptation to the light climate of the natural environment from where they were isolated [58–60], and/or to the individual evolution and selection in the laboratory growing conditions. Finally, the remarkable presence of echinenone, which content was modulated by light under N-replete condition, excludes the influence of nutrients alone on its biosynthesis.

Table 2: Summary of the pigment content, F_v/F_m, *lhcx* and *lhcr* gene expression in T-5cl6 and T-4cl3 cells under the four growth irradiances. Legend for levels: +++ (highest), ++ (high), + (moderately high), - (moderately low), -- (low), 0 (absence).

		Photophysiology	**Pigments**					**lhcx gene expression**		
		Dissipation of the light energy in excess	Photosynthetic pigments		Photoprotective pigments			Actors of NPQ	Prevent an increase in irradiance	
Strain	Light		Fx	Chl *a*	Dtx	Zx	Echinenone	*lhcx1*, *lhcx4*, *lhcx8*, *lhcx11*, *lhcr5*, *lhcr6*	*lhcx2*	*lhcx5*
T-5cl6	50 PPF	--	+++	+++	-	0	0	--	+	+++
T-4cl3		0	+++	+++	--	0	0	--	+++	-
T-5cl6	150 PPF	-	++	++	-	+	0	-	+	+
T-4cl3		--	++	++	-	0	0	+++	+	++
T-5cl6	300 PPF	+	++	+	++	++	0	+	-	-
T-4cl3		-	+	+	+	0	+	+	-	+
T-5cl6	550 PPF	++	-	-	+++	+++	0	++	--	-
T-4cl3		++	-	-	++	+	++	++	-	+

Funding:

The authors would like to acknowledge Ifremer and the Region Pays de la Loire (France) for the PhD grant of Anne Pajot. This work was co-funded by the SMIDAP through the TINAQUA project.

Acknowledgements:

The authors would like to thank Gaël Bougaran, Raymond Kaas, Jean-Baptiste Bérard, for their help with the turbidostat cultures and the sensors, Elise Robert and Agathe Maupetit, for their participation in the experiments.

Conflicts of Interest:

The authors declare no conflict of interest.

Data Availability Statement:

The original contributions presented in the study are publicly available. This data can be found here: National Center for Biotechnology Information (NCBI) BioProject database under accession number PRJNA787725.

Author contributions:

Conceptualization, A.P., E.N., T.L., J.L.; Methodology, A.P., E.N., G.C.; Formal analysis, A.P., G.C.; Investigation, A.P., J.L.; Data curation, A.P., G.C.; Writing-Original Draft preparation, A.P.; Writing-Review & Editing, J.L., E.N., G.C., T.L.; Visualization, A.P.; Supervision, E.N., L.M.; Project Administration, E.N., L.M.

6. References

[1] T. Cavalier-Smith, Chromalveolate diversity and cell megaevolution: interplay of membranes, genomes and cytoskeleton, in: Organelles, Genomes and Eukaryote Phylogeny: An Evolutionary Synthesis in the Age of Genomics, Taylor and Francis, CRC Press, 2004: pp. 71–103.

[2] A. Telfer, Singlet Oxygen Production by PSII Under Light Stress: Mechanism, Detection and the Protective role of β-Carotene, Plant and Cell Physiology. 55 (2014) 1216–1223. https://doi.org/10.1093/pcp/pcu040.

[3] A. Edreva, Generation and scavenging of reactive oxygen species in chloroplasts: a submolecular approach, Agriculture, Ecosystems & Environment. 106 (2005) 119–133. https://doi.org/10.1016/j.agee.2004.10.022.

[4] K.E. Lohman, The ubiquitous diatom - a brief survey of the present state of knowledge, American Journal of Science. 258 (1960) 180–191.
[5] M.D. Guiry, How Many Species of Algae Are There?, Journal of Phycology. 48 (2012) 1057–1063. https://doi.org/10.1111/j.1529-8817.2012.01222.x.
[6] B. Edvardsen, E.S. Egge, D. Vaulot, Diversity and distribution of haptophytes revealed by environmental sequencing and metabarcoding – a review, Pip. 3 (2016) 77–91. https://doi.org/10.1127/pip/2016/0052.
[7] C. Büchel, Light harvesting complexes in chlorophyll c-containing algae, Biochimica et Biophysica Acta (BBA) - Bioenergetics. 1861 (2020) 148027. https://doi.org/10.1016/j.bbabio.2019.05.003.
[8] A. Beer, K. Gundermann, J. Beckmann, C. Büchel, Subunit Composition and Pigmentation of Fucoxanthin−Chlorophyll Proteins in Diatoms: Evidence for a Subunit Involved in Diadinoxanthin and Diatoxanthin Binding, Biochemistry. 45 (2006) 13046–13053. https://doi.org/10.1021/bi061249h.
[9] S.-H. Zhu, B.R. Green, Photoprotection in the diatom *Thalassiosira pseudonana*: Role of LI818-like proteins in response to high light stress, Biochimica et Biophysica Acta (BBA) - Bioenergetics. 1797 (2010) 1449–1457. https://doi.org/10.1016/j.bbabio.2010.04.003.
[10] B. Lepetit, S. Sturm, A. Rogato, A. Gruber, M. Sachse, A. Falciatore, P.G. Kroth, J. Lavaud, High Light Acclimation in the Secondary Plastids Containing Diatom *Phaeodactylum tricornutum* is Triggered by the Redox State of the Plastoquinone Pool, Plant Physiology. 161 (2013) 853–865. https://doi.org/10.1104/pp.112.207811.
[11] W. Wang, L.-J. Yu, C. Xu, T. Tomizaki, S. Zhao, Y. Umena, X. Chen, X. Qin, Y. Xin, M. Suga, G. Han, T. Kuang, J.-R. Shen, Structural basis for blue-green light harvesting and energy dissipation in diatoms, Science. 363 (2019). https://doi.org/10.1126/science.aav0365.
[12] C. Büchel, Light-Harvesting Complexes of Diatoms: Fucoxanthin-Chlorophyll Proteins, in: A.W.D. Larkum, A.R. Grossman, J.A. Raven (Eds.), Photosynthesis in Algae: Biochemical and Physiological Mechanisms, Springer International Publishing, Cham, 2020: pp. 441–457. https://doi.org/10.1007/978-3-030-33397-3_16.
[13] N.L. Fisher, D.A. Campbell, J. Hughes, U. Kuzhiumparambil, K.H. Halsey, P.J. Ralph, D.J. Suggett, Divergence of photosynthetic strategies amongst marine diatoms, PLOS ONE. 15 (2020) e0244252. https://doi.org/10.1371/journal.pone.0244252.
[14] S.C. Lefebvre, G. Harris, R. Webster, N. Leonardos, R.J. Geider, C.A. Raines, B.A. Read, J.L. Garrido, Characterization and expression analysis of the Lhcf gene family in *Emiliania huxleyi* (haptophyta) reveals differential responses to light and CO2., Journal of Phycology. 46 (2010) 123–134. https://doi.org/10.1111/j.1529-8817.2009.00793.x.
[15] A. Pajot, J. Lavaud, G. Carrier, M. Garnier, B. Saint-Jean, N. Rabilloud, C. Baroukh, J.-B. Bérard, O. Bernard, L. Marchal, E. Nicolau, The Fucoxanthin Chlorophyll a/c-Binding Protein in *Tisochrysis lutea*: Influence of Nitrogen and Light on Fucoxanthin and Chlorophyll a/c-Binding Protein Gene Expression and Fucoxanthin Synthesis, Frontiers in Plant Science. 13 (2022). https://doi.org/10.3389/fpls.2022.830069.
[16] L. Blommaert, M.J.J. Huysman, W. Vyverman, J. Lavaud, K. Sabbe, Contrasting NPQ dynamics and xanthophyll cycling in a motile and a non- motile intertidal benthic diatom, Limnol. Oceanogr. 62 (2017) 1466–1479. https://doi.org/10.1002/lno.10511.
[17] B. Lepetit, G. Gélin, M. Lepetit, S. Sturm, S. Vugrinec, A. Rogato, P.G. Kroth, A. Falciatore, J. Lavaud, The diatom *Phaeodactylum tricornutum* adjusts nonphotochemical fluorescence quenching capacity in response to dynamic light via fine-tuned Lhcx and xanthophyll cycle pigment synthesis, New Phytol. 214 (2016) 205–218. https://doi.org/10.1111/nph.14337.

[18] P. Müller, X.-P. Li, K.K. Niyogi, Non-Photochemical Quenching. A Response to Excess Light Energy, Plant Physiology. 125 (2001) 1558–1566. https://doi.org/10.1104/pp.125.4.1558.
[19] S. Schaller-Laudel, D. Volke, M. Redlich, M. Kansy, R. Hoffmann, C. Wilhelm, R. Goss, The diadinoxanthin diatoxanthin cycle induces structural rearrangements of the isolated FCP antenna complexes of the pennate diatom *Phaeodactylum tricornutum*, Plant Physiology and Biochemistry. 96 (2015) 364–376. https://doi.org/10.1016/j.plaphy.2015.09.002.
[20] C. Fufezan, D. Simionato, T. Morosinotto, Identification of Key Residues for pH Dependent Activation of Violaxanthin De-Epoxidase from *Arabidopsis thaliana*, PLOS ONE. 7 (2012) e35669. https://doi.org/10.1371/journal.pone.0035669.
[21] M. Havaux, K.K. Niyogi, The violaxanthin cycle protects plants from photooxidative damage by more than one mechanism, Proc Natl Acad Sci U S A. 96 (1999) 8762–8767.
[22] H.Y. Yamamoto, T.O.M. Nakayama, C.O. Chichester, Studies on the light and dark interconversions of leaf xanthophylls, Archives of Biochemistry and Biophysics. 97 (1962) 168–173. https://doi.org/10.1016/0003-9861(62)90060-7.
[23] P. Kuczynska, M. Jemiola-Rzeminska, K. Strzalka, Photosynthetic Pigments in Diatoms, Marine Drugs. 13 (2015) 5847–5881. https://doi.org/10.3390/md13095847.
[24] P. Kuczynska, M. Jemiola-Rzeminska, B. Nowicka, A. Jakubowska, W. Strzalka, K. Burda, K. Strzalka, The xanthophyll cycle in diatom *Phaeodactylum tricornutum* in response to light stress, Plant Physiology and Biochemistry. 152 (2020) 125–137. https://doi.org/10.1016/j.plaphy.2020.04.045.
[25] M. Lohr, C. Wilhelm, Algae displaying the diadinoxanthin cycle also possess the violaxanthin cycle, Proceedings of the National Academy of Sciences. 96 (1999) 8784–8789. https://doi.org/10.1073/pnas.96.15.8784.
[26] R. Gonçalves de Oliveira-Júnior, R. Grougnet, P.-E. Bodet, A. Bonnet, E. Nicolau, A. Jebali, J. Rumin, L. Picot, Updated pigment composition of *Tisochrysis lutea* and purification of fucoxanthin using centrifugal partition chromatography coupled to flash chromatography for the chemosensitization of melanoma cells, Algal Research. 51 (2020) 102035. https://doi.org/10.1016/j.algal.2020.102035.
[27] A. Malnoë, Photoinhibition or photoprotection of photosynthesis? Update on the (newly termed) sustained quenching component qH, Environmental and Experimental Botany. 154 (2018) 123–133. https://doi.org/10.1016/j.envexpbot.2018.05.005.
[28] T. Lacour, M. Babin, J. Lavaud, Diversity in Xanthophyll Cycle Pigments Content and Related Nonphotochemical Quenching (NPQ) Among Microalgae: Implications for Growth Strategy and Ecology, Journal of Phycology. 56 (2020) 245–263. https://doi.org/10.1111/jpy.12944.
[29] T. Lacour, J. Larivière, J. Ferland, F. Bruyant, J. Lavaud, M. Babin, The Role of Sustained Photoprotective Non-photochemical Quenching in Low Temperature and High Light Acclimation in the Bloom-Forming Arctic Diatom *Thalassiosira gravida*, Frontiers in Marine Science. 5 (2018). https://www.frontiersin.org/article/10.3389/fmars.2018.00354 (accessed May 6, 2022).
[30] J. Lavaud, R. Goss, The Peculiar Features of Non-Photochemical Fluorescence Quenching in Diatoms and Brown Algae, in: Non-Photochemical Quenching and Energy Dissipation in Plants, Algae and Cyanobacteria, 2014: pp. 421–443. https://doi.org/10.1007/978-94-017-9032-1_20.
[31] K. Loubière, E. Olivo, G. Bougaran, J. Pruvost, R. Robert, J. Legrand, A new photobioreactor for continuous microalgal production in hatcheries based on external-loop airlift and swirling flow, Biotechnology and Bioengineering. 102 (2009) 132–147. https://doi.org/10.1002/bit.22035.

[32] L. Van Heukelem, C.S. Thomas, Computer-assisted high-performance liquid chromatography method development with applications to the isolation and analysis of phytoplankton pigments, Journal of Chromatography A. 910 (2001) 31–49. https://doi.org/10.1016/S0378-4347(00)00603-4.
[33] J. Berthelier, N. Casse, N. Daccord, V. Jamilloux, B. Saint-Jean, G. Carrier, Annotation of the genome assembly (version 2) of the microalga *Tisochrysis lutea*, (2018). https://doi.org/10.17882/52231.
[34] S.F. Altschul, W. Gish, W. Miller, E.W. Myers, D.J. Lipman, Basic local alignment search tool, Journal of Molecular Biology. 215 (1990) 403–410. https://doi.org/10.1016/S0022-2836(05)80360-2.
[35] W. Arsalane, B. Rousseau, J.-C. Duval, Influence of the Pool Size of the Xanthophyll Cycle on the Effects of Light Stress in a Diatom: Competition Between Photoprotection and Photoinhibition, Photochemistry and Photobiology. 60 (1994) 237–243. https://doi.org/10.1111/j.1751-1097.1994.tb05097.x.
[36] M. Lohr, C. Wilhelm, Xanthophyll synthesis in diatoms: quantification of putative intermediates and comparison of pigment conversion kinetics with rate constants derived from a model, Planta. 212 (2001) 382–391. https://doi.org/10.1007/s004250000403.
[37] K.J.M. Mulders, Y. Weesepoel, P.P. Lamers, J.-P. Vincken, D.E. Martens, R.H. Wijffels, Growth and pigment accumulation in nutrient-depleted Isochrysis aff. galbana T-ISO, J Appl Phycol. 25 (2013) 1421–1430. https://doi.org/10.1007/s10811-012-9954-6.
[38] K.J. Flynn, M. Zapata, J.L. Garrido, H. Onik, C.R. Hipkin, Changes in carbon and nitrogen physiology during ammonium and nitrate nutrition and nitrogen starvation in *Isochrysis galbana*, European Journal of Phycology. 28 (1993) 47–52. https://doi.org/10.1080/09670269300650071.
[39] S. Takaichi, M. Mochimaru, Carotenoids and carotenogenesis in cyanobacteria: unique ketocarotenoids and carotenoid glycosides, Cell. Mol. Life Sci. 64 (2007) 2607. https://doi.org/10.1007/s00018-007-7190-z.
[40] C. Punginelli, A. Wilson, J.-M. Routaboul, D. Kirilovsky, Influence of zeaxanthin and echinenone binding on the activity of the Orange Carotenoid Protein, Biochimica et Biophysica Acta (BBA) - Bioenergetics. 1787 (2009) 280–288. https://doi.org/10.1016/j.bbabio.2009.01.011.
[41] A. Wilson, G. Ajlani, J. M. Verbavatz, I. Vass, C.A. Kerfeld, D. Kirilovsky, A Soluble Carotenoid Protein Involved in Phycobilisome-Related Energy Dissipation in Cyanobacteria, Plant Cell. 18 (2006) 992–1007. https://doi.org/10.1105/tpc.105.040121.
[42] T. Kay Holt, D.W. Krogmann, A carotenoid-protein from cyanobacteria, Biochimica et Biophysica Acta (BBA) - Bioenergetics. 637 (1981) 408–414. https://doi.org/10.1016/0005-2728(81)90045-1.
[43] Y. Kusama, S. Inoue, H. Jimbo, S. Takaichi, K. Sonoike, Y. Hihara, Y. Nishiyama, Zeaxanthin and Echinenone Protect the Repair of Photosystem II from Inhibition by Singlet Oxygen in Synechocystis sp. PCC 6803, Plant and Cell Physiology. 56 (2015) 906–916. https://doi.org/10.1093/pcp/pcv018.
[44] S.B.B. Mohamad, Y.A. Yousef, T.-B. Melø, T. Jávorfi, V. Partali, H.-R. Sliwka, K. Razi Naqvi, Singlet oxygen quenching by thione analogues of canthaxanthin, echinenone and rhodoxanthin, Journal of Photochemistry and Photobiology B: Biology. 84 (2006) 135–140. https://doi.org/10.1016/j.jphotobiol.2006.02.006.
[45] B. Lepetit, D. Volke, M. Gilbert, C. Wilhelm, R. Goss, Evidence for the Existence of One Antenna-Associated, Lipid-Dissolved and Two Protein-Bound Pools of Diadinoxanthin Cycle Pigments in Diatoms, Plant Physiology. 154 (2010) 1905–1920. https://doi.org/10.1104/pp.110.166454.

[46] R. Goss, B. Lepetit, Biodiversity of NPQ, Journal of Plant Physiology. 172 (2015) 13–32. https://doi.org/10.1016/j.jplph.2014.03.004.
[47] L. Blommaert, L. Chafai, B. Bailleul, The fine-tuning of NPQ in diatoms relies on the regulation of both xanthophyll cycle enzymes, Sci Rep. 11 (2021) 12750. https://doi.org/10.1038/s41598-021-91483-x.
[48] T. Jakob, R. Goss, C. Wilhelm, Unusual pH-dependence of diadinoxanthin de-epoxidase activation causes chlororespiratory induced accumulation of diatoxanthin in the diatom *Phaeodactylum tricornutum*, Journal of Plant Physiology. 158 (2001) 383–390. https://doi.org/10.1078/0176-1617-00288.
[49] G. Yellen, The voltage-gated potassium channels and their relatives, Nature. 419 (2002) 35–42. https://doi.org/10.1038/nature00978.
[50] E.E. Pfundel, R.A. Dilley, The pH Dependence of Violaxanthin Deepoxidation in Isolated Pea Chloroplasts, Plant Physiology. 101 (93) 65–71. https://doi.org/10.1104/pp.101.1.65.
[51] J. Lavaud, A.C. Materna, S. Sturm, S. Vugrinec, P.G. Kroth, Silencing of the Violaxanthin De-Epoxidase Gene in the Diatom *Phaeodactylum tricornutum* Reduces Diatoxanthin Synthesis and Non-Photochemical Quenching, PLOS ONE. 7 (2012) e36806. https://doi.org/10.1371/journal.pone.0036806.
[52] Y. Bai, T. Cao, O. Dautermann, P. Buschbeck, M.P. Cantrell, Y. Chen, C.D. Lein, X. Shi, M.A. Ware, F. Yang, H. Zhang, L. Zhang, G. Peers, X. Li, M. Lohr, Green diatom mutants reveal an intricate biosynthetic pathway of fucoxanthin, Proc. Natl. Acad. Sci. U.S.A. 119 (2022) e2203708119. https://doi.org/10.1073/pnas.2203708119.
[53] R. Goss, E. Ann Pinto, C. Wilhelm, M. Richter, The importance of a highly active and ΔpH-regulated diatoxanthin epoxidase for the regulation of the PS II antenna function in diadinoxanthin cycle containing algae, Journal of Plant Physiology. 163 (2006) 1008–1021. https://doi.org/10.1016/j.jplph.2005.09.008.
[54] K.K. Niyogi, T.B. Truong, Evolution of flexible non-photochemical quenching mechanisms that regulate light harvesting in oxygenic photosynthesis, Current Opinion in Plant Biology. 16 (2013) 307–314. https://doi.org/10.1016/j.pbi.2013.03.011.
[55] J.M. Buck, J. Sherman, C.F. Bártulos, M. Serif, M. Halder, J. Henkel, A. Falciatore, J. Lavaud, M.Y. Gorbunov, P.G. Kroth, P.G. Falkowski, B. Lepetit, Lhcx proteins provide photoprotection via thermal dissipation of absorbed light in the diatom *Phaeodactylum tricornutum*, Nature Communications. 10 (2019) 4167. https://doi.org/10.1038/s41467-019-12043-6.
[56] M. Nymark, K.C. Valle, T. Brembu, K. Hancke, P. Winge, K. Andresen, G. Johnsen, A.M. Bones, An Integrated Analysis of Molecular Acclimation to High Light in the Marine Diatom *Phaeodactylum tricornutum*, PLOS ONE. 4 (2009) e7743. https://doi.org/10.1371/journal.pone.0007743.
[57] L. Taddei, G.R. Stella, A. Rogato, B. Bailleul, A.E. Fortunato, R. Annunziata, R. Sanges, M. Thaler, B. Lepetit, J. Lavaud, M. Jaubert, G. Finazzi, J.-P. Bouly, A. Falciatore, Multisignal control of expression of the LHCX protein family in the marine diatom *Phaeodactylum tricornutum*, EXBOTJ. 67 (2016) 3939–3951. https://doi.org/10.1093/jxb/erw198.
[58] J. Lavaud, R.F. Strzepek, P.G. Kroth, Photoprotection capacity differs among diatoms: Possible consequences on the spatial distribution of diatoms related to fluctuations in the underwater light climate, Limnology and Oceanography. 52 (2007) 1188–1194. https://doi.org/10.4319/lo.2007.52.3.1188.
[59] D. Croteau, T. Lacour, N. Schiffrine, P.-I. Morin, M.-H. Forget, F. Bruyant, J. Ferland, A. Lafond, D.A. Campbell, J.-E. Tremblay, M. Babin, J. Lavaud, Shifts in growth light optima among diatom species support their succession during the spring bloom in the

Arctic, Journal of Ecology. 110 (2022) 1356–1375. https://doi.org/10.1111/1365-2745.13874.

[60] A. Barnett, V. Méléder, L. Blommaert, B. Lepetit, P. Gaudin, W. Vyverman, K. Sabbe, C. Dupuy, J. Lavaud, Growth form defines physiological photoprotective capacity in intertidal benthic diatoms, ISME J. 9 (2015) 32–45. https://doi.org/10.1038/ismej.2014.105.

Declaration of Conflict of Interest

The authors declare that they have no known competing financial interests or personal relationships that could have appeared to inappropriately influence the work reported in this paper.

Graphical abstract

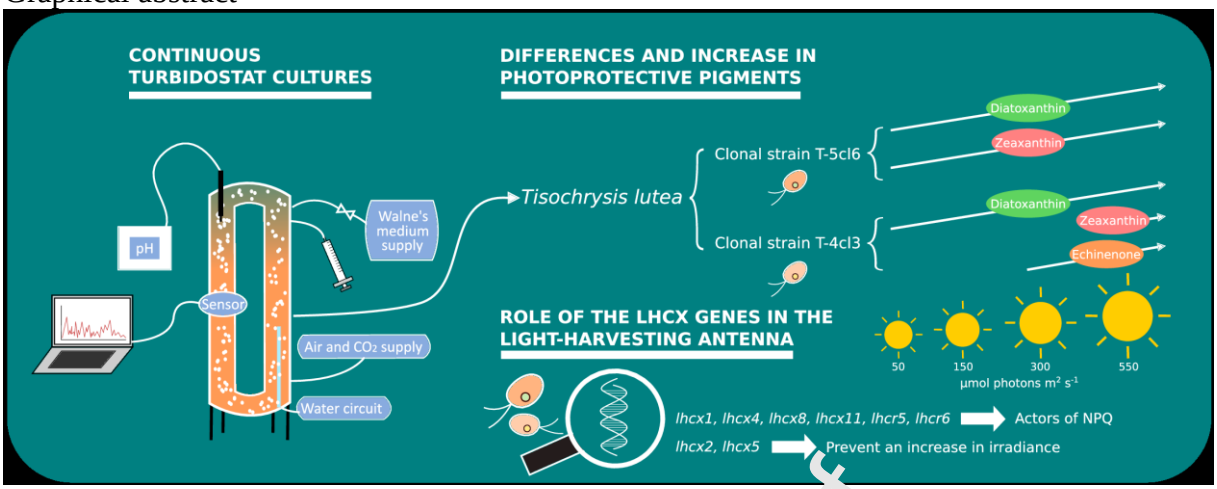

Highlights

- Continuous turbidostat cultures in triplicates were used.
- Two strains of *Tisochrysis lutea* had a different photoprotection strategy.
- Echinenone was remarkably accumulated in one strain under high light.
- Four genes involved in de-epoxidation and epoxidation were annotated.
- *lhcx*, *lhcr* and *lhcf* participate in the fine photosynthesis/photoprotection balance.